PAPER

Temperature-dependent phonon dynamics and anharmonicity of suspended and supported few-layer gallium sulfide

View the article online for updates and enhancements.

Temperature-dependent phonon dynamics and anharmonicity of suspended and supported few-layer gallium sulfide

Francisco D V Araujo[1,2] , Victor V Oliveira[3] , Andreij C Gadelha[4] ,
Thais C V Carvalho[5], Thales F D Fernandes[4] , Francisco W N Silva[6] , R Longuinhos[7] ,
Jenaina Ribeiro-Soares[7] , Ado Jorio[4] , Antonio G Souza Filho[8] , Rafael S Alencar[3]
and Bartolomeu C Viana[1,5]

[1] Pós-Graduação em Ciência e Engenharia dos Materiais, Universidade Federal do Piauí, Teresina, Piauí,
64049-550, Brazil
[2] Instituto Federal de Educação, Ciência e Tecnologia do Piauí-IFPI, 64760-000, Piauí, Brazil
[3] Faculdade de Física, Universidade Federal do Pará, Belém, Pará, 66075-110 Brazil
[4] Departamento de Física, Universidade Federal de Minas Gerais, Belo Horizonte, Minas Gerais,
30270-901 Brazil
[5] Departamento de Física, Universidade Federal do Piauí, Teresina, Piauí, 64049-550, Brazil
[6] Instituto Federal de Educação, Ciência e Tecnologia do Maranhão-Campus Alcântara, Alcântara,
Maranhão, Brazil
[7] Departamento de Física, Universidade Federal de Lavras, Lavras, Minas Gerais, 37200-000, Brazil
[8] Departamento de Física, Centro de Ciências, Universidade Federal do Ceará, Fortaleza, Ceará,
60455-900, Brazil

E-mail: bartolomeu@ufpi.edu.br

CrossMark

Abstract

Phonons play a fundamental role in the electronic and thermal transport of 2D materials which
is crucial for device applications. In this work, we investigate the temperature-dependence of
A_{1g}^1 and A_{1g}^2 Raman modes of suspended and supported mechanically exfoliated few-layer
gallium sulfide (GaS), accessing their relevant thermodynamic Grüneisen parameters and
anharmonicity. The Raman frequencies of these two phonons soften with increasing temperature
with different $\theta = \partial\omega/\partial T$ temperature coefficients. The first-order temperature coefficients θ of
A_{1g}^2 mode is ~ -0.016 cm^{-1}/K, independent of the number of layers and the support. In
contrast, the θ of A_{1g}^1 mode is smaller for two-layer GaS and constant for thicker samples
($\sim -0.006\,2$ cm^{-1} K^{-1}). Furthermore, for two-layer GaS, the θ value is $\sim -0.004\,4$ cm^{-1} K^{-1}
for the supported sample, while it is even smaller for the suspended one ($\sim -0.002\,9$ cm^{-1}
K^{-1}). The higher θ value for supported and thicker samples was attributed to the increase in
phonon anharmonicity induced by the substrate surface roughness and Umklapp phonon
scattering. Our results shed new light on the influence of the substrate and number of layers on
the thermal properties of few-layer GaS, which are fundamental for developing atomically-thin
GaS electronic devices.

1. Introduction

Nowadays, a rich plethora of two-dimensional (2D) layered materials beyond graphene have drawn intense interest due to their novel physical properties [1–5]. Research regarding 2D materials is in a growing trend, and many new materials are inserted into their group every year. Thus, the rich library of 2D materials group can consist of more than 150 types up to date [6]. The 2D materials can be categorized based on their structure, like graphene, hexagonal boron nitride (h-BN), transition metal dichalcogenides or TMDs, with the MX_2 formula (e.g. MoS_2, WS_2, $MoSe_2$ and WSe_2), black phosphorous, layered double hydroxides (LDHs), a group of mono-elemental compounds (Xenes), metal oxides, graphitic carbon nitride (g-C_3N_4), metal nitrides/carbides (MXenes), transition metal halides (TMHs) (e.g. PbI_2 and $MgBr_2$), transition metal oxides (e.g. MnO_2 and MoO_3), perovskite-type oxides (e.g. $K_2Ln_2Ti_3O_{10}$ and $RbLnTa_2O_7$ (Ln: lanthanide ion), and 2D polymers [6].

Graphene-like two-dimensional (2D) layered materials constitute an important family of crystals that cover a large range of optoelectronic properties for different devices [3, 7, 8]. Furthermore, the development of new synthesis and exfoliation methods have promoted the isolation of many interesting monolayers 2D materials, which exhibit unusual electronic, thermal, mechanical, and chemical properties, such as the TMDs [9–16], phosphorene [17], silicene [18–22], germanene [23–25], stanene [26], borophene [27] and gallene [28].

In particular, the bulk post-transition metal monochalcogenide GaS is an indirect semiconductor with band gap of 2.5 eV [29–32], which can be tuned by reducing the crystal thickness [31], similar to other 2D systems [11, 33, 34]. The GaS crystal structure is built up from the stacking of S-Ga-Ga-S (one-layer, or one atomic quadrilayer) layers via weak van der Waals forces, thus forming a β polytype structure [35]. Because of its special physics properties (flexible material [36], wide bandgap [37], tunable electronic properties by varying the GaS thickness or applaying strain [38] and high photoresponse [29, 32], for example) GaS is promising for applications in photoelectric devices and electrical sensors [39].

In general, the prospects of applications of new 2D materials are fundamentally dependent on their thermal properties [40–43]. For instance, to promote a high-performance on electronic devices, an efficient heat dissipation is necessary, while a low heat dissipation is preferred in thermoelectric applications [44, 45]. Thus, the understanding of few-layered GaS thermal transport properties is extremely needed and only

recently started to be addressed [46]. From this point of view, phonons play a crucial role in electronic transport and carrier dynamics of 2D materials for next-generation nanoelectronic device applications [47].

In order to understand the phonon properties in 2D systems, it is important to correlate them to the transport properties, the electron-phonon and phonon-phonon interactions, which in turn, are related to the performance of electronic devices due to non-harmonic effects in the lattice potential energy [48]. Particularly, scattering by optical phonons has been observed to limit electrical transport and heat dissipation [49, 50]. Therefore, by probing the changes introduced by temperature on Raman signatures of few-layer GaS can give us information about its thermal properties [46, 51–53].

Raman spectroscopy is a non-destructive technique for characterizing 2D layered materials. It has been widely used to estimate the number of atomic layers, to probe mechanical and thermal properties of these systems [41, 42, 54–58], since phonons can be used as a tool for probing temperature- [59] and pressure- [60, 61] induced biaxial strain. Furthermore, Raman measurement is performed without special sample treatment and shape requirement [46]. In particular, Jastrzebski *et al* [46] have developed an analytical function to determine the GaS layer thickness from Raman measurements. However, other techniques (HRTEM and AFM) can be used to determine the thickness of 2D materials [46, 62–66], but it is necessary the deterministic transference of the samples and cross-section preparation to the HRTEM grids, or a very rigorous treatment of the surface to eliminate residues for AFM measurements which can generate errors of the thickness measurements of the sample.

The thermal properties of suspended and supported transition metal dichalcogenides materials have been reported previously, thus showing the influence of the substrate [42, 56–58]. For few-layer GaS samples, there is only one study reporting the phonon anharmonicity for supported four- and seven-layer GaS [46]. Thus, to the best of our knowledge, temperature-dependent Raman spectroscopy studies of two-, three- and multi-layer GaS samples (suspended and supported) have not been reported yet, being their thermal dependence important for future GaS-based applications.

In this paper, we investigate the temperature effect on the Raman spectra of suspended and supported two-, three- and multi-layer GaS samples obtained by mechanical exfoliation. The first-order temperature coefficient $\theta = \partial\omega/\partial T$ was estimated for each A_{1g} Raman mode by using a three-phonon process (a phonon decaying into two other phonons). The differences in the phonon anharmonicity were associated with both the scattering of phonons by the surface roughness of the

substrate and the enhancement of Umklapp scattering with the increasing number of GaS layers. Our results provide fundamental information about the thermal properties of few-layer GaS, which is useful for designing electronic applications.

2. Sample and experimental setup

Few-layer GaS were obtained by standard mechanical exfoliation [67] from a single-crystal source (provided by **2D semiconductors**), deposited on a cleaned SiO_2/Si substrate with holes of ~ 3 μm, through the stamp transfer method [68]. The 200 nm thicker SiO_2 layer on top of the Si substrate was chosen to obtain a good optical contrast to identify the thinnest GaS layers. After the deposition of thin GaS samples onto the SiO_2/Si substrate, the thinnest flakes were initially identified by optical microscopy, shown in figure 1(a). The thinnest samples are slightly different in contrast from the substrate. Next, the ultrathin layers of GaS on SiO_2/Si were measured using non-destructive Raman spectroscopy as presented in figure 1(b) and (c), being the Raman measurements performed without any special sample preparation.

Raman experiments were performed using a Bruker Senterra system and a Horiba T6400 microscope-based spectrometer (in the triple mode), both equipped with the 2.33 eV (532 nm) excitation energy laser source. The power level was 300 mW outside of the laser and ~ 145 μW at the outlet of the 100x objective lens to acquire the Raman spectra at room temperature. For the high and low temperatures experiments the power level used was 20 mW outside the laser and ~ 50 μW at the outlet of the 50x objective lens. The typical integration time used was 10 accumulations of 15 seconds. The Raman signal was dispersed by a grating of 1800 grooves/mm, resulting in a spectral resolution of ~ 1 cm^{-1}. A 100x objective lens with a numeric aperture of NA = 0.9 (WD = 0.21 mm) was used to focus the laser beam and to collect the Raman signal in a backscattering geometry [69, 70] at room temperature Raman experiments, while for temperature-dependent measurements was used a long work distance (WD = 18 mm) 50x objective lens with NA = 0.35.

The high- and low-temperature was achieved by a Linkam thermal stage THMS600, which was purged with argon gas under normal pressure. The argon atmosphere was applied to prevent sample oxidation at high temperatures. However, the temperature measured by the cryostat controller can differ from the temperature at the sample. Thus, we used the Si Raman peak ($\sim$ 520.5 cm^{-1} at room temperature [71]) as a sensor of temperature at the few-layer GaS. A comparison of the main results with the temperature scale measured by the cryostat controller is summarized in figures S1-S3 and table S1 of the supplementary information (stacks.iop.org/NANO/31/495702/mmedia). As we can see, the temperature measured by the Si peak differs considerably from the temperature measured by the controller, especially in high temperatures. The hole size in the SiO_2/Si substrate is large enough (3 μm) to guarantee the extraction of the suspended GaS thermal dependence with high accuracy since the hole diameter is larger than the largest laser beam spot size (< 2 μm)

used. We cleaned the SiO_2/Si substrate following the recipe: ultrasound cleaning in acetone followed by isopropanol baths for two minutes each, and blow dry using argon. We prepared ourselves the three-micron hole patterns by optical lithography and chemical etching in BOE solution. After the etching procedure, we clean the patterned substrate using oxygen plasma, getting rid of resist residues.

The Raman measurements were performed on three different positions of the same flake for two-, three- and multi-layer GaS. It is noteworthy mentioning that any flake with suspended one-layer GaS was not observed.

3. Results and discussions

Figure 1(a) shows an optical image of the GaS flake deposited on top of the holes (~ 3 μm diameter size) of the drilled SiO_2/Si substrate. The brighter the area, the thicker the sample. The colorful dots mark the positions where the Raman measurements were performed.

The Raman spectrum of bulk GaS is characterized by the following phonon frquencies (irreducible representations): 22.8 cm^{-1} (E_{2g}^2), 74.7 cm^{-1} (E_{1g}^1), 189 cm^{-1} (A_{1g}^1), 291.8 cm^{-1} (E_{1g}^2), 295.8 cm^{-1} (E_{2g}^1) and 360.9 cm^{-1} (A_{1g}^2) [72, 73]. Our Raman analysis are focused only on the most intense modes A_{1g}^1 and A_{1g}^2. The analysis of the E_{2g}^1 mode is difficult due to its frequency overlap with the silicon substrate's 2TA mode (303 cm^{-1}) [46] and its intensity is very low when the GaS thickness decreases [72, 74].

Figure 1(b) shows the Raman spectra of supported GaS flake (P_{out}) recorded at room temperature and at different positions on the sample, as well as the spectrum of the GaS bulk crystal reference. For clarity, all spectra were normalized by the A_{1g}^1 mode intensity and vertically shifted. The intensities of both A_{1g} modes and the A_{1g}^1 Raman frequency ($\omega_{A_{1g}^1}$) decrease when the number of layers decreases, while the A_{1g}^2 Raman frequency ($\omega_{A_{1g}^2}$) is almost constant.

Jastrzebski *et al* [46] have studied the GaS Raman spectrum as a function of number of layers. They correlate the $\omega_{A_{1g}^1}$ with the GaS thickness and proposed an analytical exponential function to determine the layer thickness from Raman measurements. In this sense, we fit each Raman mode of figure 1(b) with one Voigt component and plot the $\omega_{A_{1g}^1}$ with the exponential function proposed by Jastrzebski, as shown in figure 1(c). Alencar *et al* have shown new Raman active modes emerging at Raman shifts near to those bulk Raman modes, with A_{1g} and E_{2g} symmetries in the few-layer limit, some of them being observed as 'shoulders' in the experimental data [72]. These new phonon modes present Raman tensors with components similar to those observed in bulk. Thus, the Voigt function is used here in a way that its Gaussian component accounts for these new Raman active modes emerging at Raman shifts near to those A_{1g} modes and the response function of the spectrometer, which is considered to be a gaussian [46, 73]. It is worth mentioning that we used the $\omega_{A_{1g}^1}$ of bulk GaS measured in this work. Thus, the number of layers of the three regions studied
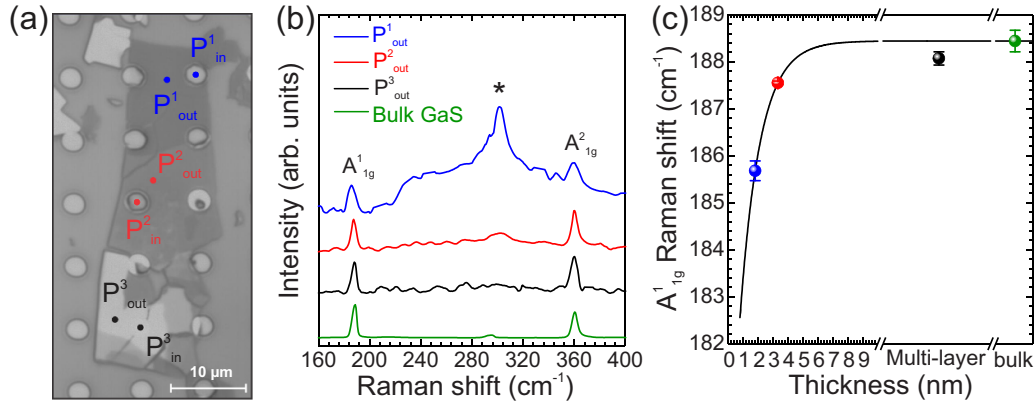
Figure 1. (a) Optical image of the GaS flake on drilled SiO$_2$/Si substrate. (b) Raman spectra collected at three different regions (colorful P$_{out}$ dots) on the GaS flake and on the reference crystal sample. (c) A$^1_{1g}$ Raman shift as a function of GaS thickness fitted with an exponential function $\omega_{A^1_{1g}} = 188.443 - 10.67 e^{-0.744h}$ proposed by Jastrzebski *et al* [46]. Here *h* is the GaS thickness in nm. The peak marked with * comes from the Si/SiO$_2$ substrate.

here were classified as follow: P1 = 2 layers, P2 = 3 layers and P3 = multi-layer.

Temperature-dependent Raman measurements of suspended and supported GaS samples were performed in the temperature range of 148–614 K. Figures 2 (a)–(f) show normalized Raman spectra of two-layer, tri-layer and multi-layer GaS samples collected on suspended and supported regions (P$_{in}$ and P$_{out}$ dots in figure 1(a)) at different temperatures. The Raman modes were fitted with Voigt functions and the temperature-dependence of A$^1_{1g}$ and A$^2_{1g}$ frequencies are plotted in figure 3. As expected, the modes red-shift with increasing temperature, similar to what has been observed in other 2D materials [42, 43, 56, 75–78].

The purely anharmonic contribution to the A$_{1g}$ Raman shift can be modeled through the phonon decay Balkanski's approach [71]:

$$\omega(T) = \omega_0 + A\left[1 + \frac{2}{e^x - 1}\right] + B\left[1 + \frac{3}{e^y - 1} + \frac{3}{(e^y - 1)^2}\right],$$ (1)

where $x = \frac{\hbar\omega_0}{2k_BT}$, $y = \frac{\hbar\omega_0}{3k_BT}$, T is the absolute temperature, k_B is the Boltzmann's constant, $\omega(T)$ is the wavenumber at T and ω_0 is the wavenumber at 0 K. The A and B parameters are related to contributions of three-phonon and four-phonon processes to the frequency shifts.

The linear behavior observed in figure 3 has also been observed in others 2D materials for supported and suspended samples [42, 43, 56, 57, 75–79]. This linear trend for both A$_{1g}$ modes indicates that the three-phonon process is dominant in the temperature range measured. For $x \ll 1$ (i.e. for high temperatures) the equation (1) tends to a linear dependence:

$$\omega(T) = \omega_0 + \theta T; \; \theta \approx \frac{4K_B}{\hbar\omega_0}A$$ (2)

where θ is the first-order temperature coefficient $\frac{\partial\omega}{\partial T}$.

In this work the temperature-dependence of the A$_{1g}$ modes were fitted using the equation (2). The θ parameters for two-, three- and multi-layer GaS are shown in table 1. Since there is

a considerable difference in the temperature measured by the controller thermal stage and the Si Raman peak methodology, a comparison with θ values reported by Jastrzebski *et al* [46] is not appropriate.

The Grüneisen parameter γ is an important thermodynamic quantity which describes changes in cell volume induced by temperature and pressure variations. It indicates the anharmonic effects on the phonon spectrum: the higher γ, the higher anharmonicity. The isobaric mode Grüneisen parameter γ_P and θ are related via the following equation [52, 53]:

$$\gamma_P = -\frac{1}{\alpha\omega_0}\theta,$$ (3)

where ω_0 is defined in equation (1) and estimated from the experimental data. α parameter is the thermal expansion coefficient. Since there is no report on the thermal expansion for few-layer GaS, we use the in-plane α value (at 300 K) from bulk GaS [52, 78, 80] in order to calculate γ_P. The results are shown in table 1. Figure 4 summarizes the dependence of γ_P on the number of layers for A$^1_{1g}$ and A$^2_{1g}$ for suspended and supported samples. The isobaric mode Grüneisen parameter of the A$^2_{1g}$ mode is nearly independent of the number of layers and also whether the sample is supported or not, especially if the uncertainty is taken into account, see figure 4. On the other hand, the γ_P parameter of A$^1_{1g}$ mode is smaller for the two-layer GaS and becomes constant for thicker samples. Moreover, the γ_P is smaller for suspended two-layer GaS compared to the supported one. It is worth mentioning that a comparison of the intrinsic anharmonicity found here (for suspended few-layer GaS with other 2D systems) needs information of γ_P of suspended samples with the same number of layers. Thus, we will focus only on discussing the effect of substrate and number of layers on GaS anharmonicity.

A similar result has been observed by Carvalho *et al* [78] for suspended and supported one-layer WSe$_2$. They attributed the higher γ_P value for A$_{1g}$ phonon in supported WSe$_2$ as being
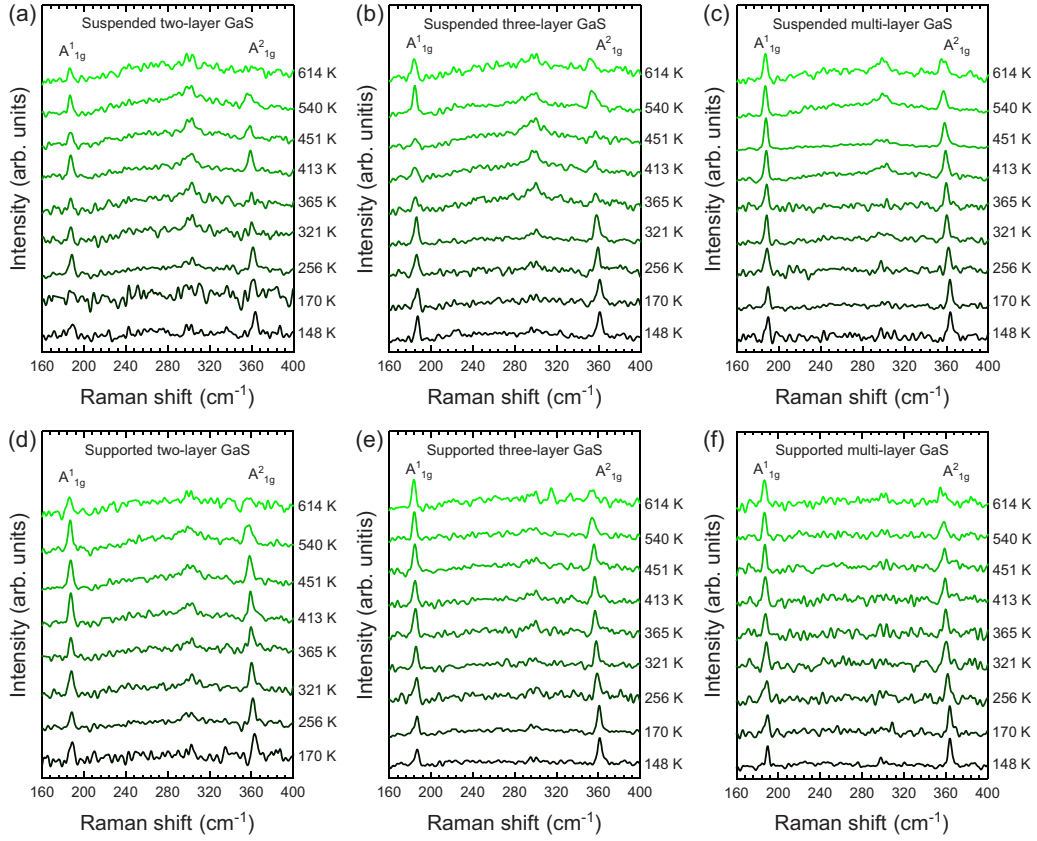
Figure 2. (a)–(c) Normalized Raman spectra of suspended (acquired at the positions P_{in}^1, P_{in}^2, and P_{in}^3 respectively) and (d)–(f) supported (acquired at the positions P_{out}^1, P_{out}^2, and P_{out}^3 respectively) two-, three and multi-layer GaS recorded at different temperatures.

Table 1. A_{1g} mode Raman shift at T = 0 K (ω_0), the first-order temperature coefficient (θ)and the isobaric mode Grüneisen parameter (γ_P) of supported and suspended few-layer GaS.

Sample	Vibrational mode	ω_0 (cm^{-1})	θ (cm^{-1}/K)	γ_P
		Two-layer GaS		
Suspended	A_{1g}^1	188.3 ± 0.2	−0.002 9 ± 5.5x10^{-4}	1.17 ± 0.22
	A_{1g}^2	365.6 ± 0.4	−0.016 3 ± 1.2x10^{-3}	3.33 ± 0.24
Supported	A_{1g}^1	189.2 ± 0.2	−0.004 4 ± 4.3x10^{-4}	1.72 ± 0.17
	A_{1g}^2	365.1 ± 0.4	−0.014 6 ± 1.2x10^{-3}	2.99 ± 0.24
		Three-layer GaS		
Suspended	A_{1g}^1	187.6 ± 0.1	−0.006 5 ± 3.6x10^{-4}	2.61 ± 0.14
	A_{1g}^2	363.4 ± 0.2	−0.016 9 ± 7.6x10^{-4}	3.48 ± 0.15
Supported	A_{1g}^1	187.6 ± 0.1	−0.006 5 ± 2.5x10^{-4}	2.63 ± 0.10
	A_{1g}^2	363.5 ± 0.2	−0.016 7 ± 6.5x10^{-4}	3.44 ± 0.13
		Multi-layer GaS		
Suspended	A_{1g}^1	190.0 ± 0.1	−0.005 3 ± 2.8x10^{-4}	2.08 ± 0.11
	A_{1g}^2	365.9 ± 0.2	−0.016 1 ± 4.3x10^{-4}	3.30 ± 0.09
Supported	A_{1g}^1	190.3 ± 0.2	−0.006 5 ± 5.8x10^{-4}	2.56 ± 0.23
	A_{1g}^2	366.4 ± 0.2	−0.016 9 ± 6.7x10^{-4}	3.45 ± 0.14

due to the increase of the phonon anharmonicity induced by the phonon scattering with the surface roughness of the substrate. For few-layer supported GaS, Alencar *et al* [81] has attributed the higher phonon correlation length (L$_c$) measured for A_{1g}^1 compared to the A_{1g}^2 as being due to the superior A_{1g}^2

anharmonicity. Besides, a decrease in thermal conductivity κ (which is proportional to γ^{-2} [82]) with increasing number of layers in MoS$_2$, MoSe$_2$ and graphene was attributed to a greater phase space for Umklapp phonon scattering in thicker samples, resulting from crystal anharmonicity [41, 42, 83].
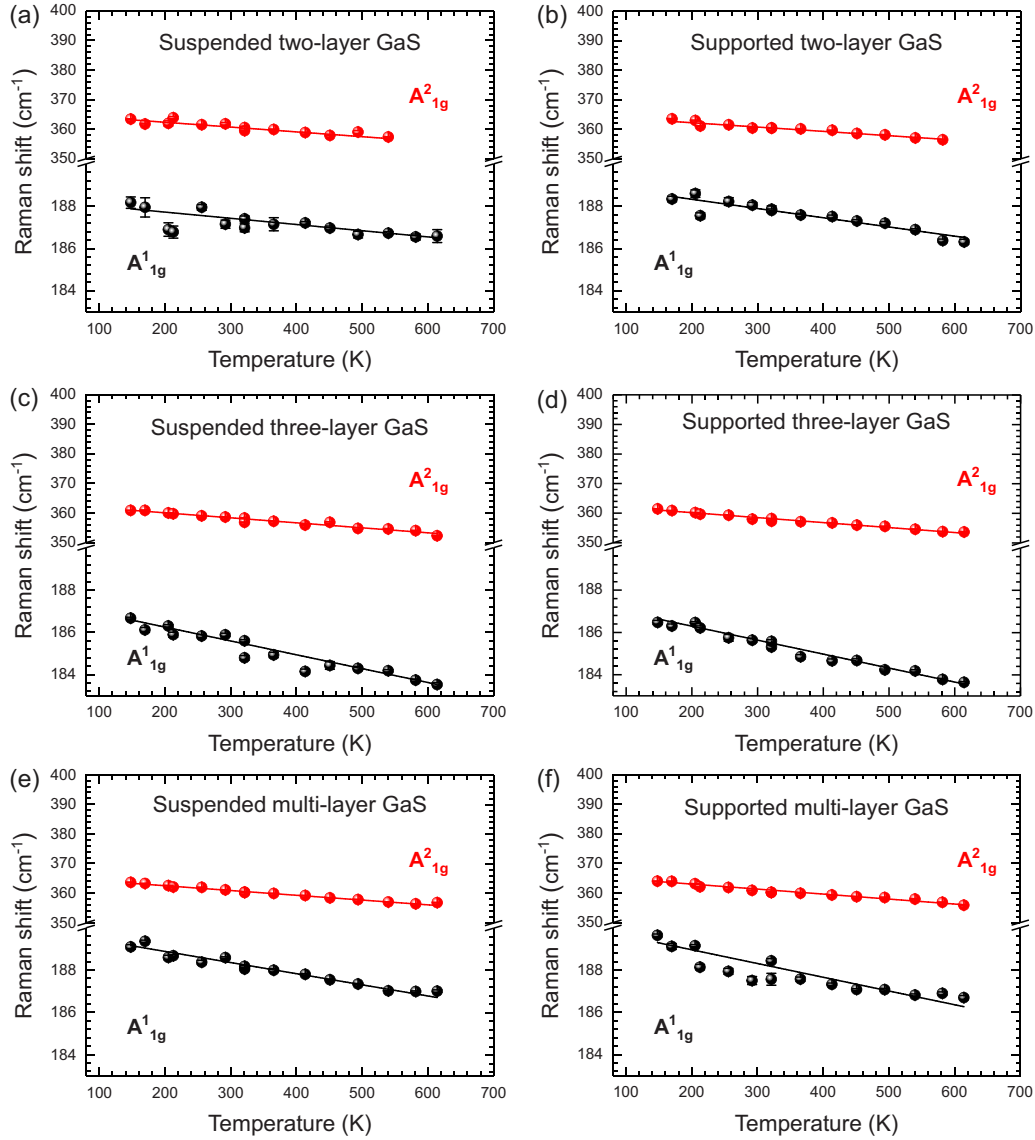
Figure 3. Temperature-dependence of the A_{1g} Raman shift of suspended (a), (c) and (e) and supported (b), (d) and (f) two-, three- and multi-layer GaS. The linear fitting parameters for experimental data are listed in table I.

In this sense, the higher γ_P value for A_{1g}^1 mode found in supported two-layer GaS compared to suspended one is attributed to the increase in phonon anharmonicity caused by the scattering of the phonon with the surface roughness of the substrate. In contrast, since the A_{1g}^2 mode has superior anharmonicity (lower L_c) the phonon scattering with substrate surface roughness is not dominant and noticed, in fully agreement with model reported in reference [81]. For three- and multi-layer GaS the higher γ_P is assigned to the enhancement in phonon anharmonicity induced by both substrate surface roughness and Umklapp phonon scattering promoted by the higher number of layers. It is worth mentioning that the influence of in-plane biaxial strain was not accounted for in our methodology and it can influence the Raman peak shift. Thus, the temperature coefficient and the isobaric mode Grüneisen parameters calculated here could slightly differ from a real free-standing GaS sample.

4. Conclusions

In summary, we performed a temperature-dependent Raman study of the optical A_{1g}^1 and A_{1g}^2 phonons of suspended and supported two-, three, and multi-layer GaS. Our results show a linear frequency decreasing for both A_{1g} modes with increasing temperature and the first-order temperature coefficients θ were calculated by considering the three-phonon process anharmonicity. For the A_{1g}^2 mode, θ is estimated to be ~ -0.016 cm^{-1}/K and independent of the number of layers and the sample support, while for A_{1g}^1 mode θ is smaller for two-layer GaS and constant for thicker samples (~ -0.0062 cm^{-1}/K). Also, for two-layer GaS a smaller θ value for suspended sample (~ -0.0029 cm^{-1}/K), compared to θ for the supported one (~ -0.0044 cm^{-1}/K), is observed. We attributed the higher θ value calculated for supported and thicker samples as being due to the enhancement
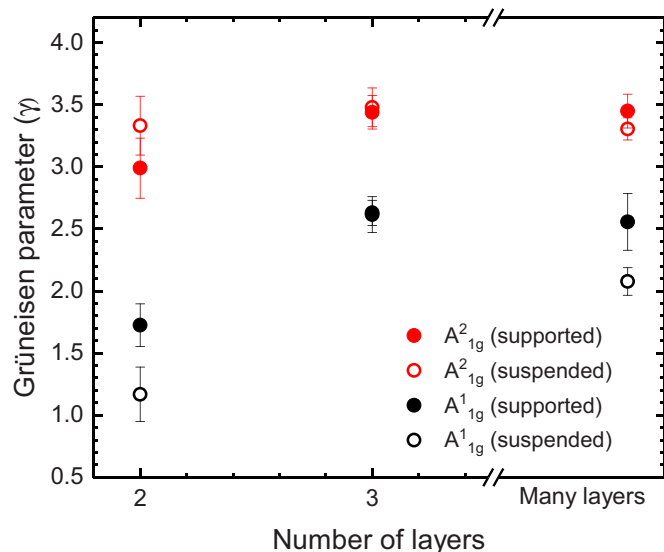
Figure 4. A_{1g}^1 (black symbols) and A_{1g}^2 (red symbols) isobaric mode Grüneisen parameters as function of GaS number of layers for suspended (empty symbols) and supported (filled symbols).

in phonon anharmonicity induced by substrate surface roughness and Umklapp phonon scattering. Our experimental results provide an understanding of the influence of the substrate and the number of layers on the thermal properties of few-layer GaS, and the methodology used here can be extended to other 2D systems.

Acknowledgments

ORCID iDs

Francisco D V Araujo
ⓘ https://orcid.org/0000-0002-2257-3374
Victor V Oliveira
ⓘ https://orcid.org/0000-0003-2149-6335
Andreij C Gadelha
ⓘ https://orcid.org/0000-0002-6350-7680
Thales F D Fernandes
ⓘ https://orcid.org/0000-0003-3868-9029
Francisco W N Silva
ⓘ https://orcid.org/0000-0002-3241-3059
R Longuinhos
ⓘ https://orcid.org/0000-0003-1615-4672
Jenaina Ribeiro-Soares
ⓘ https://orcid.org/0000-0001-9248-2243
Ado Jorio
ⓘ https://orcid.org/0000-0002-5978-2735
Antonio G Souza Filho
ⓘ https://orcid.org/0000-0003-3802-1168
Rafael S Alencar
ⓘ https://orcid.org/0000-0002-9992-7564
Bartolomeu C Viana
ⓘ https://orcid.org/0000-0002-5207-4269

References

[1] Basov D N, Fogler M M and García de Abajo F J 2016 *Science* **354**
[2] Novoselov K S, Mishchenko A, Carvalho A and Castro Neto A H 2016 *Science* **353**
[3] Das S, Robinson J A, Dubey M, Terrones H and Terrones M 2015 *Ann. Rev. Mater. Res.* **45** 1–27
[4] Xia F, Wang H and Jia Y 2014 *Nat. Commun.* **5** 4458
[5] Guo Y *et al* 2018 *Sci. Adv.* **4**
[6] Khan K, Tareen A K, Aslam M, Wang R, Zhang Y, Mahmood A, Ouyang Z, Zhang H and Guo Z 2020 *J. Mater. Chem.* C **8** 387–440
[7] Li X L, Han W P, Wu J B, Qiao X F, Zhang J and Tan P H 2017 *Adv. Funct. Mater.* **27** 1604468
[8] Bhimanapati G R *et al* 2015 *Recent Advances in Two-Dimensional Materials beyond Graphene*
[9] Lee C, Yan H, Brus L E, Heinz T F, Hone J and Ryu S 2010 *ACS Nano* **4** 2695–700
[10] Mak K F, Lee C, Hone J, Shan J and Heinz T F 2010 *Phys. Rev. Lett.* **105** 136805
[11] Splendiani A, Sun L, Zhang Y, Li T, Kim J, Chim C Y, Galli G and Wang F 2010 *Nano Lett.* **10** 1271–5
[12] Smith R J *et al* 2011 *Adv. Mater.* **23** 3944–8
[13] Lee Y H *et al* 2012 *Adv. Mater.* **24** 2320–5
[14] Zhan Y, Liu Z, Najmaei S, Ajayan P M and Lou J 2012 *Small* **8** 966–71
[15] Liu K K *et al* 2012 *Nano Lett.* **12** 1538–44
[16] Gong Y *et al* 2015 *ACS Nano* **9** 11658–66
[17] Li L, Yu Y, Ye G J, Ge Q, Ou X, Wu H, Feng D, Chen X H and Zhang Y 2014 *Nat. Nanotechnol.* **9** 372–7
[18] Aufray B, Kara A, Vizzini S, Oughaddou H, Léandri C, Ealet B and Le Lay G 2010 *Appl. Phys. Lett.* **96** 183102
[19] Feng B, Ding Z, Meng S, Yao Y, He X, Cheng P, Chen L and Wu K 2012 *Nano Lett.* **12** 3507–11
[20] De Padova P, Kubo O, Olivieri B, Quaresima C, Nakayama T, Aono M and Le Lay G 2012 *Nano Lett.* **12** 5500–3

[21] Vogt P, De Padova P, Quaresima C, Avila J, Frantzeskakis E, Asensio M C, Resta A, Ealet B and Le Lay G 2012 *Phys. Rev. Lett.* **108** 155501

[22] Tao L, Cinquanta E, Chiappe D, Grazianetti C, Fanciulli M, Dubey M, Molle A and Akinwande D 2015 *Nat. Nanotechnol.* **10** 227–31

[23] Dávila M E, Xian L, Cahangirov S, Rubio A and Lay G L 2014 *New J. Phys.* **16** 095002

[24] Bianco E, Butler S, Jiang S, Restrepo O D, Windl W and Goldberger J E 2013 *ACS Nano* **7** 4414–21

[25] Derivaz M, Dentel D, Stephan R, Hanf M C, Mehdaoui A, Sonnet P and Pirri C 2015 *Nano Lett.* **15** 2510–16

[26] Zhu F-F, Chen W, Xu Y, Gao C, Guan D, Liu C, Qian D, Zhang S C and Jia J 2015 *Nat Mater.* **14** 1020–5

[27] Sachdev H 2015 *Science* **350** 1468–9

[28] Kochat V *et al* 2018 *Sci. Adv.* **4**

[29] Hu P *et al* 2013 *Nano Lett.* **13** 1649–54

[30] Xu M, Liang T, Shi M and Chen H 2013 *Chem. Rev.* **113** 3766–98

[31] Jung C S, Shojaei F, Park K, Oh J Y, Im H S, Jang D M, Park J and Kang H S 2015 *ACS Nano* **9** 9585–93

[32] Yang S, Li Y, Wang X, Huo N, Xia J B, Li S S and Li J 2014 *Nanoscale* **6** 2582–7

[33] Tonndorf P *et al* 2013 Photoluminescence emission and Raman response of MoS2, MoSe 2 and WSe2 nanolayers *Conf. on Lasers and Electro-Optics, CLEO 2013* IEEE Computer Society vol 21 pp 4908–16

[34] Zhao W, Ghorannevis Z, Chu L, Toh M, Kloc C, Tan P H and Eda G 2013 *ACS Nano* **7** 791–7

[35] Irwin J, Hoff R, Clayman B and Bromley R 1973 *Solid State Commun.* **13** 1531–6

[36] Yagmurcukardes M, Senger R T, Peeters F M and Sahin H 2016 *Phys. Rev.* B **94** 245407

[37] Late D J, Liu B, Matte H S S R, Rao C N R and Dravid V P 2012 *Adv. Functional Mater.* **22** 1894–905

[38] Ma Y, Dai Y, Guo M, Yu L and Huang B 2013 *Phys. Chem. Chem. Phys.* **15** 7098–105

[39] Shen G, Chen D, Chen P C and Zhou C 2009 *ACS Nano* **3** 1115–20

[40] Gonnelli R S *et al* 2015 *Sci. Rep.* **5** 9554

[41] Ghosh S, Bao W, Nika D L, Subrina S, Pokatilov E P, Lau C N and Balandin A A 2010 *Nat. Mater.* **9** 555–8

[42] Zhang Y, Sun D, Li Y, Lee G H, Cui X, Chenet D, You Y, Heinz T F and Hone J C 2015 *ACS Appl. Mater. Interfaces* **7** 25923–9

[43] Vieira A G *et al* 2016 *Vib. Spectrosc.* **86** 270–6

[44] Yalon E *et al* 2017 *Nano Lett.* **17** 3429–33

[45] Fu Y *et al* 2019 *2D Mater.* **7** 012001

[46] Jastrzebski C, Olkowska K, Jastrzebski D J, Wierzbicki M, Gebicki W and Podsiadlo S 2019 *J. Phys.: Condens. Matter.* **31**

[47] Sangwan V K and Hersam M C 2018 *Annu. Rev. Phys. Chem.* **69** 299–325 pMID: 29463170

[48] Tristant D, Cupo A, Ling X and Meunier V 2019 *ACS Nano* **13** 10456–68

[49] Berciaud S, Han M Y, Mak K F, Brus L E, Kim P and Heinz T F 2010 *Phys. Rev. Lett.* **104** 227401

[50] Tian Z, Esfarjani K, Shiomi J, Henry A S and Chen G 2011 *Appl. Phys. Lett.* **99** 053122

[51] Peng B, Zhang H, Shao H, Xu Y, Zhang X and Zhu H 2016 *RSC Adv.* **6** 5767–73

[52] Yang M, Cheng X, Li Y, Ren Y, Liu M and Qi Z 2017 *Appl. Phys. Lett.* **110** 093108

[53] Bhatt S V, Deshpande M P, Sathe V, Rao R and Chaki S H 2014 *J. Raman Spectrosc.* **45** 971–9

[54] Cai W, Moore A L, Zhu Y, Li X, Chen S, Shi L and Ruoff R S 2010 *Nano Lett.* **10** 1645–51

[55] Gutiérrez H R *et al* 2013 *Nano Lett.* **13** 3447–54

[56] Sahoo S, Gaur A P, Ahmadi M, Guinel M J and Katiyar R S 2013 *J. Phys. Chem* **117** 9042–7

[57] M T and Late D J 2014 *ACS Appl. Mater. Interfaces* **6** 1158–63

[58] Thripuranthaka M, Kashid R V, Sekhar Rout C and Late D J 2014 *Appl. Phys. Lett.* **104**

[59] Plechinger G, Castellanos-Gomez A, Buscema M, van der Zant H S J, Steele G A, Kuc A, Heine T, Schüller C and Korn T 2015 *2D Mater.* **2** 015006

[60] Machon D, Bousige C, Alencar R, Torres-Dias A, Balima F, Nicolle J, de Sousa Pinheiro G, Souza Filho A G and San-Miguel A 2018 *J. Raman Spectrosc.* **49** 121–9

[61] Alencar R S, Saboia K D, Machon D, Montagnac G, Meunier V, Ferreira O P, San-Miguel A and Souza Filho A G 2017 *Phys. Rev. Mater.* **1** 024002

[62] Norimatsu W and Kusunoki M 2014 *Phys. Chem. Chem. Phys.* **16** 3501–11

[63] Laskar M R, Ma L, Kannappan S, Sung Park P, Krishnamoorthy S, Nath D N, Lu W, Wu Y and Rajan S 2013 *Appl. Phys. Lett.* **102** 252108

[64] Tan L K, Liu B, Teng J H, Guo S, Low H Y and Loh K P 2014 *Nanoscale* **6** 10584–8

[65] Kim J H, Ko T J, Okogbue E, Han S S, Shawkat M S, Kaium M G, Oh K H, Chung H S and Jung Y 2019 *Sci. Rep.* **9** 1641

[66] Rubino S, Akhtar S and Leifer K 2016 *Microscopy Microanalysis* **22** 250–6

[67] Novoselov K S and Neto A H C 2012 *Phys. Scr.* 014006

[68] Castellanos-Gomez A, Buscema M, Molenaar R, Singh V, Janssen L, van der Zant H S J and Steele G A 2014 *2D Mater.* **1** 011002

[69] Larkin P 2011 Chapter 3 - Instrumentation and Sampling Methods *Infrared and Raman Spectroscopy* ed Larkin P (Oxford: Elsevier) pp 27–54

[70] Ferraro J R, Nakamoto K and Brown C W 2003 *Chapter 2 - Instrumentation and Experimental Techniques Introductory Raman Spectroscopy* 2nd edn ed Ferraro J R, Nakamoto K and Brown C W (San Diego: Academic) pp 95–146

[71] Balkanski M, Wallis R F and Haro E 1983 *Phys. Rev.* B **28** 1928–34

[72] Alencar R S, Longuinhos R, Rabelo C, Miranda H L S, Viana B C, Souza Filho A G, Cancado L G, Jorio A and Ribeiro-Soares J 2020 *unpublished*

[73] Gasanly N M, Aydinli A, Özkan H and Kocabas C 2000 *Solid State Commun.* **116** 147–51

[74] Zhang X, Tan Q H, Wu J B, Shi W and Tan P H 2016 *Nanoscale* **8** 6435–50

[75] Yan R *et al* 2014 *ACS Nano* **8** 986–93

[76] Peimyoo N, Shang J, Yang W, Wang Y, Cong C and Yu T 2015 *Nano Res.* **8** 1210–21

[77] Lanzillo N A *et al* 2013 *Appl. Phys. Lett.* **103**

[78] Carvalho T C *et al* 2019 *AIP Adv.* **9** 085316

[79] Balandin A A, Ghosh S, Bao W, Calizo I, Teweldebrhan D, Miao F and Lau C N 2008 *Nano Lett.* **8** 902–7

[80] Belenkii G, Abdullayeva S, Solodukhin A and Suleymanov R 1982 *Solid State Commun.* **44** 1613–15

[81] Alencar R S *et al* 2019 *Nano Lett.* 7357–64

[82] Slack G 1973 *J. Phys. Chem. Solids* **34** 321–35

[83] Balandin A A 2011 *Nat. Mater.* **10** 569-81